FDG-PET in tau-negative amnestic dementia resembles that of autopsy-proven hippocampal sclerosis

18 authors, including:

Hugo Botha
Mayo Foundation for Medical Education and Research
75 PUBLICATIONS **565** CITATIONS

SEE PROFILE

Melissa E. Murray
Mayo Clinic
277 PUBLICATIONS **9,860** CITATIONS

SEE PROFILE

Christopher G. Schwarz
Mayo Foundation for Medical Education and Research
169 PUBLICATIONS **1,993** CITATIONS

SEE PROFILE

Some of the authors of this publication are also working on these related projects:

REM Sleep Behavior Disorder View project

Alzheimer's disease View project

FDG-PET in tau-negative amnestic dementia resembles that of autopsy-proven hippocampal sclerosis

Hugo Botha,[1],* William G. Mantyh,[1],* Melissa E. Murray,[2] David S. Knopman,[1] Scott A. Przybelski,[3] Heather J. Wiste,[3] Jonathan Graff-Radford,[1] Keith A. Josephs,[1] Christopher G. Schwarz,[4] Walter K. Kremers,[5] Bradley F. Boeve,[1] Ronald C. Petersen,[1] Mary M. Machulda,[6] Joseph E. Parisi,[7] Dennis W. Dickson,[2] Val Lowe,[4] Clifford R. Jack, Jr[4] and David T. Jones[1,4]

*These authors contributed equally to this work.

Predicting underlying pathology based on clinical presentation has historically proven difficult, especially in older cohorts. Age-related hippocampal sclerosis may account for a significant proportion of elderly participants with amnestic dementia. Advances in molecular neuroimaging have allowed for detailed biomarker-based phenotyping, but in the absence of antemortem markers of hippocampal sclerosis, cases of mixed pathology remain problematic. We evaluated the utility of ^{18}F-FDG-PET to differentiate flortaucipir tau PET negative from flortaucipir positive amnestic mild cognitive impairment and dementia and used an autopsy confirmed cohort to test the hypothesis that hippocampal sclerosis might account for the observed pattern. We identified impaired participants (Clinical Dementia Rating > 0) with amnestic presentations ⩾ 75 years who had MRI and PET imaging with ^{18}F-FDG (glucose metabolism), Pittsburgh compound B (amyloid) and flortaucipir (tau) performed within a year of cognitive assessment. These were stratified into amyloid positive/negative and tau positive/negative according to the A/T/N classification scheme. Our sample included 15 amyloid and tau-positive participants, and nine tau-negative participants (five of whom were amyloid-positive). For the autopsy cohort, sequential cases with antemortem ^{18}F-FDG-PET were screened and those with TDP-43-negative Alzheimer's disease (10 cases) and TDP-43-positive hippocampal sclerosis (eight cases) were included. We compared each group to controls and to each other in a voxel-based analysis, and supplemented this with a region of interest-based analysis comparing medial to inferior temporal metabolism. Tau-positive and negative cases did not differ on neuropsychological testing or structural magnetic resonance biomarkers. Tau-negative cases had focal medial temporal and posterior cingulate/retrosplenial hypometabolism regardless of amyloid status, whereas tau-positive cases had additional lateral parietal and inferior temporal involvement. The inferior/medial temporal metabolism ratio was significantly different between the groups with the tau-negative group having a higher ratio. In the autopsy series, hippocampal sclerosis cases had greater medial temporal hypometabolism than Alzheimer's disease cases, who had more parietal and lateral/inferior temporal hypometabolism. Again, the ratio between temporal regions of interest differed significantly between groups. Two of the tau-negative patients, both of whom had an elevated inferior/medial temporal ratio, came to autopsy during the study and were found to have hippocampal sclerosis. Our finding that tau-negative amnestic mild cognitive impairment and dementia is associated with focal medial temporal and posterior cingulate hypometabolism extends prior reports in amyloid-negative cases. The inferior/medial temporal metabolism ratio can help identify tau-negative cases of amnestic dementia and may serve as a biomarker for hippocampal sclerosis.

1 Department of Neurology, Mayo Clinic, Rochester, Minnesota, 55905, USA
2 Department of Anatomic Pathology, Mayo Clinic, Jacksonville, Florida, 32224, USA
3 Department of Biomedical Statistics and Informatics, Mayo Clinic, Rochester, Minnesota, 59905 USA
4 Department of Radiology, Mayo Clinic, Rochester, Minnesota, 55905, USA
5 Department of Health Sciences Research, Rochester, Minnesota, 55905, USA
6 Department of Psychiatry and Psychology, Rochester, Minnesota, 55905, USA
7 Department of Neuropathology, Mayo Clinic, Rochester, Minnesota, 55905, USA

Correspondence to: David T. Jones, MD
Department of Neurology,
Mayo Clinic, 200 First St SW, Rochester, MN 55905, USA
E-mail: Jones.David@mayo.edu

Introduction

Among degenerative pathologies that may mimic or co-exist with Alzheimer's disease in elderly patients, hippocampal sclerosis of ageing (hereafter simply hippocampal sclerosis) may be a significant contributor. Given their predominant impairment in memory, during life the majority of hippocampal sclerosis cases are diagnosed clinically with Alzheimer's disease dementia (Nelson et al., 2011). It is one of the limbic predominant non-Alzheimer's pathologies that is frequently seen in amnestic mild cognitive impairment (MCI) (Petersen et al., 2006). Prevalence estimates range from 5 to 30% among those with advanced old age (Nelson et al., 2011). Hippocampal sclerosis is also often seen in association with Alzheimer's disease pathology, with estimates ranging anywhere from 2 to 20% (Zarow et al., 2008; Nelson et al., 2011; Mortimer, 2012; Josephs et al., 2014), with a higher proportion seen in cases of limbic predominant Alzheimer's disease. Furthermore, whereas Alzheimer's disease appears to plateau in the 80s or 90s, the prevalence of hippocampal sclerosis continues to rise with increasing age and among the oldest old may be more prevalent than Alzheimer's disease (Dickson et al., 1994; Tyas et al., 2007; Nelson et al., 2011; Mortimer, 2012). It is increasingly being recognized as a major contributor to late life memory loss, and in the current era of targeted therapy development, *in vivo* prediction of the underlying pathology has become paramount for appropriate therapeutic trial enrolment (Nelson et al., 2012). Despite the increased focus on hippocampal sclerosis, and its frequently associated proteinopathy TAR DNA-binding protein 43 (TDP-43, encoded by *TARDBP*) there are no reliable hippocampal sclerosis biomarkers, and antemortem diagnosis has hence been difficult.

Although it is no substitute for amyloid or tau PET imaging, FDG-PET may prove useful in defining tau-negative amnestic dementia and exploring possible *in vivo* signs of hippocampal sclerosis. While FDG-PET hypometabolism closely (inversely) mirrors tau PET in persons in the Alzheimer's disease spectrum (Ossenkoppele et al., 2016),

FDG-PET is a non-specific marker of neurodegeneration. We sought to use it to identify non-Alzheimer's neurodegenerative diseases such as hippocampal sclerosis in which FDG and tau PET are dissociated. Our study examined the utility of FDG-PET in identifying non-Alzheimer's causes of amnestic MCI or dementia in elderly ($\geqslant$75 years of age) participants. We began with the assumption that cognitively impaired tau PET negative individuals had a pathological process other than Alzheimer's disease as the primary cause of the impairment, although Alzheimer's disease may still play a role. First, we compared the patterns of hypometabolism among tau-negative amnestic participants who were amyloid-positive (A+/T−) versus amyloid-negative (A−/T−). The participants who were T− displayed the same FDG-PET pattern whether they were A+ or A−, and as such we combined them into one group (T−). We then compared these tau-negative participants (A±/T−) with tau-positive amnestic participants (A+/T+), and identified a pattern that appeared to be associated with tau status. To test the hypothesis that this pattern may be representative of underlying hippocampal sclerosis, we used the same imaging techniques in a separate cohort of autopsy-proven TDP-43 positive hippocampal sclerosis cases compared to TDP-43 negative Alzheimer's disease cases with no hippocampal sclerosis. Finally, two of the clinical tau-negative participants came to autopsy during the study. Both were accurately predicted to have hippocampal sclerosis based on the molecular imaging results and the pattern of hypometabolism, and are discussed in more detail.

Materials and methods

Participants

Clinical cohort

Participants were from the Mayo Clinic Alzheimer's Disease Research Center and the Mayo Clinic Study of Aging (Roberts et al., 2008). We identified all participants who met the

following criteria: the participant had at least one tau PET, amyloid PET, FDG-PET and structural MRI performed within a year of a clinical assessment; the participant was deemed cognitively impaired (Clinical Dementia Rating >0) according to the behavioural neurologist who evaluated the participant; and the participant was 75 years or older at the time of imaging. The age restriction was motivated by prior studies that reported a median age of onset of 75–79 in cases of hippocampal sclerosis, as well as the fact that hippocampal sclerosis is rare in participants that die before the age of 80 (Nelson *et al.*, 2013; Murray *et al.*, 2014). Furthermore, when we extended our search to those below the age of 75 only one additional patient clinically suspected of having Alzheimer's disease but with negative flortaucipir imaging (standard uptake value ratio, SUVR < 1.33) was identified (Supplementary Table 1). On further review this patient had extratemporal flortaucipir binding. This is in contrast to the negative flortaucipir subjects over the age of 75 that had no evidence of extra temporal PET signal. As such, we felt our age cut-off was justified based on tau-negative amnestic dementia and MCI being primarily a problem in those aged 75 years or older. All of these cases were reviewed and those who had amnestic MCI or amnestic dementia suspected to be due to Alzheimer's disease at a consensus meeting of neuropsychologists and behavioural neurologists were included (Albert *et al.*, 2011; McKhann *et al.*, 2011). Of note, biomarkers were not considered during this diagnostic classification. Patients who met criteria for probable dementia with Lewy bodies or who had clear evidence of REM sleep behavioural disorder were excluded (McKeith *et al.*, 2017), as were those who met criteria for non-amnestic dementia syndromes, such as behavioural variant frontotemporal dementia (Piguet *et al.*, 2011), atypical variants of Alzheimer's disease such as posterior cortical atrophy (Tang-Wai *et al.*, 2004) or any of the primary progressive aphasia variants (Gorno-Tempini *et al.*, 2004). We also excluded participants where a primary psychiatric disorder or use of sedating medications was thought to explain their cognitive complaints. Participants whose imaging failed quality control measures or who had evidence of large hemispheric strokes were also excluded. This cohort was then matched (2:1) for age and sex with a control cohort of cognitively normal and biomarker-negative participants from the Mayo Clinic Study of Aging (Roberts *et al.*, 2008). Participants were grouped according to tau biomarker status, as outlined below, for purposes of imaging and statistical analyses.

Standard protocol approvals, registrations and patient consents

This study was approved by the Mayo Clinic institutional review board and written consent was obtained from all participants and/or their qualified representative in keeping with the Declaration of Helsinki.

Neuropsychological testing

Participants completed a comprehensive neuropsychological battery as part of the Uniform Data Set designed by the National Alzheimer's Coordinating Center (Monsell *et al.*, 2016). Data from the following tests were abstracted: Montreal Cognitive Assessment, Craft Story Immediate and Delayed Recall (both verbatim and paraphrase recall),

Benson Figure Copy and Recall, Multilingual Naming Test, Category fluency (Animals and Vegetables), Digit Span Length forwards, Trial Making Test Part B. Test scores were then converted to z-scores controlling for age, sex and education using the z-score calculator on the National Alzheimer's Coordinating Center website (https://www.alz.washington.edu/WEB/npsych_means.html).

Structural imaging

MRI was performed on one of three 3 T systems from the same vendor. Hippocampal volumes were quantified using Freesurfer, and adjusted for total intracranial volume from SPM12 (Jack *et al.*, 2017). Structural MRI was used for pre-processing PET data, and spatially normalized and modulated grey matter intensities derived from SPM12 (http://www.fil.ion.ucl.ac.uk/spm/software/spm12/) were used in the region of interest-based analysis described below.

Amyloid and tau PET imaging

Amyloid PET imaging was done with Pittsburgh compound B, synthesized on-site with precursor purchased from ABX Biochemical Compounds. Tau PET was carried out with flortaucipir (AV-1451), synthesized on-site with precursor supplied by Avid Radiopharmaceuticals. Late-uptake amyloid PET images were acquired 40–60 min, and tau PET 80–100 min, after injection. Although flortaucipir uptake does not appear to plateau, a delayed image during the 80–100-min window has been shown to be reliable for cortical structures (Shcherbinin *et al.*, 2016; Barret *et al.*, 2017). A CT scan was obtained for attenuation correction. Methods of PET data analysis have been described previously (Jack *et al.*, 2012). Briefly, an SUVR was derived for amyloid PET from the voxel size weighted median uptake in the prefrontal, orbitofrontal, parietal, temporal, anterior and posterior cingulate, and precuneus regions of interest normalized to the cerebellar grey median. For tau PET, the voxel size weighted median uptake from a meta-region of interest consisting of the entorhinal, amygdala, parahippocampal, fusiform, inferior temporal, and middle temporal regions of interest normalized to the median uptake in the cerebellar crus was used to derive the SUVR. The hippocampus is not included in this region of interest because of frequent bleed from the adjacent choroid plexus. Although the best regions to use for quantifying tau PET uptake and the best cut-off point to use in binary classification schemes are an active topic of research, this meta-region of interest is similar to those used by other groups (Mishra *et al.*, 2017). Further details regarding the design and justification of the meta-region of interest can be found elsewhere (Jack *et al.*, 2017). Grey and white matter sharpening was applied, whereby voxels whose probability of being CSF was greater than the probability of being grey matter or white matter based on co-registered segmented MRI are excluded from the SUVR calculation.

We had previously examined several different methods for selecting cut-off points to define abnormality with amyloid PET and tau PET (Jack *et al.*, 2017). The optimum amyloid PET cut-off point of SUVR 1.42 was based on the threshold value beyond which the rate of change in amyloid PET reliably increases. We determined the cut-off point for tau PET by maximizing the accuracy (i.e. maximizing sensitivity plus specificity) in discriminating between amyloid-positive individuals with MCI or dementia versus Mayo Clinic Study of Aging

cognitively unimpaired, age-matched individuals. Based on this method, the cut-off point for tau PET was 1.33 SUVR. Based on the amyloid and tau cut-off points each participant was designated as amyloid positive or negative (A+/A−) and tau positive or negative (T+/T−) as recommended by the A/T/N classification scheme (Jack *et al.*, 2016*a*).

Autopsy cohort

The autopsy cohort was constructed from a consecutive series of autopsy participants who had antemortem FDG-PET imaging performed. As part of a standardized dissection and sampling protocol (Terry *et al.*, 1987), formalin-fixed and paraffin-embedded sections of the left hemisphere were taken for immunohistochemical studies. Plaques and neurofibrillary tangles were assessed for using thioflavin-S fluorescent microscopy (Murray *et al.*, 2011) and staged in accordance with recommendation from the National Institute of Aging-Alzheimer's Association (NIA-AA) and Consortium to Establish a Registry for Alzheimer's disease (CERAD) guidelines (Mirra *et al.*, 1991; Hyman *et al.*, 2012). Immunohistochemistry was performed with antibodies against tau, TDP-43 and alpha-synuclein. Hippocampal sclerosis was diagnosed in the setting of neuronal loss in CA1 and the subiculum that was judged to be out of proportion to the neurofibrillary tangle pathology burden, according to consensus recommendations (Rauramaa *et al.*, 2013). Participants with TDP-43-positive hippocampal sclerosis (hereafter 'hippocampal sclerosis') were identified, regardless of whether or not co-existing Alzheimer's disease was present. A subset of Alzheimer's disease participants with no evidence of TDP-43 or alpha-synuclein were identified as a comparison cohort (hereafter 'Alzheimer's disease'). The same structural and FDG-PET processing and analyses were applied to this group.

FDG-PET imaging and analysis

All patients had FDG-PET images acquired using a PET/CT scanner (GE Healthcare) operating in 3D mode. Patients were injected in a dimly lit room with ^{18}F-FDG, and after a 30-min uptake period, an 8-min FDG scan was performed, which consisted of four 2-min dynamic frames following a low dose CT transmission scan. PET image processing was done using our fully automated, in-house pipeline, described previously (Senjem *et al.*, 2005). Briefly, after co-registration of MRI and PET images for each patient, the automated anatomical labelling (AAL) atlas was propagated to native MRI space and the pons was identified (Tzourio-Mazoyer *et al.*, 2002). PET image intensity was normalized to the pons and smoothed with an 8 mm full-width at half-maximum Gaussian kernel, after which all voxels were divided by the median uptake in the pons. The parameters from MRI normalization were used to normalize these FDG-uptake ratio images to template space (Vemuri *et al.*, 2008). Results were assessed with and without partial volume correction (PVC) using a two-compartment model, as outlined by Meltzer *et al.* (1999). This involves combining the grey and white matter segmentations into a tissue probability mask, resampling this to the approximate resolution of FDG-PET by smoothing it with a 6 mm full-width at half-maximum Gaussian filter and then dividing the smoothed PET images by the smoothed brain tissue probability mask. In effect, the PET values in voxels with intermediate probability to contain brain tissue (e.g. 0.5) are boosted,

whereas the values in voxels that are more confidently assigned to brain (e.g. 0.99) or not brain (e.g. 0.01) are not changed significantly. However, PVC for FDG-PET images is different than amyloid or tau PET in an important way: in FDG-PET the signal of interest usually decreases with disease state and stage (i.e. reduced metabolism in affected regions) whereas in amyloid and tau PET the signal increases with progression. Because PVC either increases signal intensity or leaves it unchanged the net effect is that it tends to reduce power to detect group differences, and at times destroys an effect that is known to be there (e.g. in simulation cases) (Greve *et al.*, 2016). As such, we focused our analyses on the non-PVC images. Group level analyses of normalized and scaled FDG-PET images were performed using SPM12 (http://www.fil.ion. ucl.ac.uk/spm/software/spm12/). Voxel-level comparisons of FDG-PET images for each diagnostic group were compared to controls in SMP12 using a one-sided *t*-test and to each other with two-sided *t*-tests. A conjunction analysis was done in SPM using the amyloid-positive and amyloid-negative groups within the tau-negative group in order to identify areas that are involved in both amyloid-positive and amyloid-negative participants (Price and Friston, 1997; Price *et al.*, 1997). Results were viewed uncorrected ($P = 0.001$) and corrected for multiple comparisons [family wise error (FWE) correction $P = 0.05$].

Given the small numbers, the direct disease group differences did not reach statistical significance. T-maps were converted to effect size (Cohen's *d*) maps. To quantify the pattern observed in the effect size maps at a single participant level, and to allow for a summary metric that could be applied to other cohorts, we created two regions of interest based on the AAL atlas (Tzourio-Mazoyer *et al.*, 2002). Since the medial temporal lobe was more involved in tau-negative cases, we chose to combine the hippocampus and amygdala AAL regions of interest to form a 'medial temporal' region of interest. We also used the 'inferior temporal' AAL region of interest given the inferior temporal involvement in tau-positive cases. After masking the PET image of each participant with their spatially normalized and modulated grey matter intensity map, such that only voxels with > 0.5 probability of being grey matter were included, the median FDG uptake ratio for each region of interest was calculated for each participant. The ratio of inferior temporal/medial temporal metabolism was then calculated and used to compare controls, tau-positive and tau-negative participants. We then used the same region of interest and ratio and applied it to the autopsy cohort, whose group imaging findings were not taken into account when the regions of interest were selected, to test the ability of the ratio to separate hippocampal sclerosis from Alzheimer's disease cases.

Given that atrophy may account for some of the hypometabolism observed on FDG-PET, we performed a similar region of interest-based analysis using Freesurfer thicknesses for inferior temporal and entorhinal regions of interest based on the Freesurfer atlas (Freesurfer 5.3, available from http://surfer. nmr.mgh.harvard.edu/) (Fischl *et al.*, 2002, 2004; Han and Fischl, 2007).

Finally, we used the 3D stereotactic surface projections generated with CortexID (GE Healthcare) to view the participant level FDG-PET scans. This is a propriety processing and presentation suite that is used in clinical practice at our institution. After a fully automated preprocessing procedure, which includes realignment, spatial normalization and non-linear

warping, 16 000 predefined cortical locations which are sampled and then projected onto a 3D brain surface. Participant PET data are normalized to the pons and compared to a normative database, resulting in a 3D stereotactic surface projections Z-score image.

Statistical analysis

All statistical analysis was done in R (Version 3.4.1). The Mann-Whitney-Wilcoxon test was used for continuous variables, including imaging-derived metrics, while chi-square test was used for categorical variables such as sex. Fisher's exact was used for *APOE* genotype given the small numbers. Voxel-wise imaging analysis was done in SPM as outlined above.

Results

Clinical cohort

Our initial search identified 47 participants, 23 of whom were excluded. See Supplementary Table 2 for a list of excluded patients and their associated amyloid-PET and

tau-PET status. The remaining 24 participants all presented with an amnestic syndrome and met criteria for amnestic MCI (n = 8) or Alzheimer's disease dementia (n = 16) on consensus review. Nine participants were tau-negative, of which five were amyloid-positive and four were amyloid-negative. The remaining 15 participants were positive on both biomarkers. Tau-negative participants were older than tau-positive participants, and tau-positive participants were more likely to carry an *APOE ε4* allele (67% versus 28%), although the difference did not reach significance (P = 0.1597). No group differences were found in neuropsychological test performance (Table 1).

Autopsy cohort

Eighteen participants were included in the autopsy cohort. Eight participants had TDP-43 positive hippocampal sclerosis, with co-existing Alzheimer's pathology seen in most cases. Two hippocampal sclerosis participants had alpha-synuclein positive inclusions isolated to the amygdala, with negative staining elsewhere, including the anterior and posterior cingulate cortices and the brainstem. The

Table 1 Demographic and neuropsychologic test results for each patient group

	A−/T−/N+ (n = 4)	A+/T−/N+ (n = 5)	All T−/N+ (n = 9)	A+/T+/N+ (n = 15)	P-value
Sex, % male	0	80	44	47	0.9158
Education (Q1, Q3)	15 (13.5, 16)	16 (16, 16)	16 (14, 16)	16 (14, 19.5)	0.3397
Age at PET (Q1, Q3)	82 (79, 85)	85 (81, 89)	85 (79, 86)	76 (75, 78.5)	0.0031
APOE genotype					
ApoE4 carriers, (%)[a]	1/4 (25)	1/3 (33)	2/7 (28)	9/13 (67)	0.1597
Global function					
MoCA (Q1, Q3)	17 (13.5,19)	16 (13, 16)	16 (13, 19)	15 (8.5, 21)	0.7879
MMSE (Q1, Q3)	22 (16.5, 22.75)	24 (24, 26)	24 (22, 25)	22 (19, 25)	0.6969
CDR Global (Q1, Q3)	1 (0.75, 1)	0.5 (0.5, 1)	0.75 (0.5, 1)	1 (0.5, 1)	0.312
CDR Sum of Boxes (Q1, Q3)	6 (4.5,6.5)	2.5 (0.5, 5.5)	4.25 (2, 6)	4.5 (3.5, 9)	0.2559
Language function					
Multilingual Naming Test, z-score (Q1, Q3)	0.25 (0, 0.5)	−3.3 (−4.9, −0.2)	−0.18 (−3.7, 0.1)	−2.15 (−3.1, −1.3)	0.4088
Category Fluency, z-score (Q1, Q3)	−1.71 (−2, −1.7)	−1.85 (−2, −1.34)	−1.78 (−2.1, −1.6)	−1.76 (−2.4, −1.1)	0.9039
Memory function					
Craft Story, Immediate Recall, z-score (Q1, Q3)	−1.93 (−2.2, −1.5)	−2.72 (−3, −2.1)	−2.29 (−2.8, −1.7)	−2.27 (−2.5, −1.6)	0.8404
Craft Story, Delayed Recall, z-score (Q1, Q3)	−2.35 (−2.8, −2)	−2.72 (−2.8, −2.5)	−2.62 (−2.8, −2.2)	−2.93 (−3.2, −2.5)	0.1483
Benson Diagram, Delayed Recall, z-score (Q1, Q3)	−2.82 (−3.2, −2.5)	−2.36 (−3.2, −2.1)	−2.59 (−3.3, −2.2)	−3.48 (−3.7, −2.9)	0.1087
Attention/Executive function					
Digit Span, Forward, z-score (Q1, Q3)	−0.59 (−0.84, −0.37)	0.12 (−0.11, 0.26)	−0.36 (−0.4, 0.1)	−0.41 (−0.9, 0.2)	0.6983
Trial Making Test Part B, z-score (min, max)	−3.86[b]	−1.08 and 0.00[b]	−1.08 (−3.9, 0.0)	−1.02 (−5.3, 0.29)	1
Visuospatial function					
Benson Diagram, Copy, z-score (Q1, Q3)	1.13 (−0.8,1.3)	−1.00 (−2.6, 1)	0.01 (−2.6, 1.1)	−0.40 (−1.9, −0.4)	0.5631
Molecular imaging					
Amyloid SUVR	1.33 (1.30, 1.35)	2.01 (1.57, 2.03)	1.54 (1.34, 2.01)	2.71 (2.56, 2.84)	0.0017
Tau SUVR	1.20 (1.14, 1.26)	1.26 (1.24, 1.29)	1.26 (1.14, 1.27)	1.62 (1.59, 1.94)	<0.0001

Demographic and neuropsychological test results for each patient group. Z-scores, corrected for age, sex, and education, are shown for individual cognitive domains. Median and interquartile range (Q1, Q3) are reported unless stated otherwise. Each cognitive domain is tested in accordance with the Uniform Data Set version 3.0 neuropsychological battery. The first two columns report results for tau-negative participants split by amyloid status. These are combined in column 3 and compared with tau-positive participants. P-values shown are for the tau-positive versus tau-negative group comparison.
[a]Two patients from the tau PET negative (T−/N+) group and two patients from the tau PET positive (T+/N+) group were missing *APOE* genotyping.
[b]Missing for multiple participants, participant level result(s) shown.
MMSE = Mini-Mental State Examination; A+ = amyloid-PET positive; A− = amyloid-PET negative; MoCA = Montreal Cognitive Assessment; T−/N+ = tau-PET negative, neurodegeneration positive; T+/N+ = tau-PET positive, neurodegeneration positive.

remaining 10 participants had Alzheimer's disease and no evidence of hippocampal sclerosis or TDP-43 deposition. Demographics and additional neuropathological details for this cohort are shown in Table 2. No significant difference was found between hippocampal sclerosis and Alzheimer's disease cases in age or disease duration at time of PET imaging or at death.

Voxel-wise FDG-PET

Clinical cohort

Results for tau-negative participants split by amyloid status compared to controls are shown in Fig. 1. Both amyloid-negative and amyloid-positive participants had hypometabolism involving the medial temporal lobes, posterior cingulate and the adjacent precuneus bilaterally, with sparing of the inferior and lateral temporal lobes. A direct comparison between these groups did not reveal any differences, and the conjunction analysis confirmed overlapping hypometabolism involving the regions mentioned previously. Because this FDG pattern appeared to be independent of amyloid status, we combined the amyloid-positive and amyloid-negative participants who did not have elevated tau into one group for further analyses.

Table 2 Demographic and pathology data for autopsy cohort

	Hippocampal sclerosis (*n* = 8)	Alzheimer's disease (*n* = 10)
Demographics		
Sex, male/female	3/5	7/3
Age at FDG-PET (Q1, Q3)	83 (79.25, 84.75)	83 (79.25, 84.75)
Duration at FDG-PET (Q1, Q3)[a]	7 (2.5, 9)	7.5 (6, 9.75)
Age at death (Q1, Q3)	89 (86.75, 93)	87.5 (82.5, 89.5)
Level of Alzheimer's disease pathological changes		
Not Alzheimer's	1	0
Low	0	0
Intermediate	5	3
High	2	7
ABC		
A0B1C0	1	0
A3B5C2	2	1
A3B6C2	0	2
A4B3C2	1	0
A4B4C2	2	0
A4B6C2	0	1
A5B5C2	1	1
A5B6C2	1	5

Count data are reported, except for age and duration where median and interquartile range (Q1, Q3) are reported. There were no statistically significant differences for sex (*P* = 0.3416), age at PET (*P* = 0.4449), duration at PET (*P* = 0.5168) or age at death (*P* = 0.2289) between groups. The level of Alzheimer's disease neuropathological change and ABC staging are reported according to NIA-AA guidelines (Hyman *et al.*, 2012).
[a]Data not available for four Alzheimer's disease and one hippocampal sclerosis participants.

Results for tau-negative and tau-positive participants compared to controls and to each other are shown in Fig. 2. The tau-negative participants had hypometabolism limited to the regions discussed above, whereas the tau-positive participants had prominent involvement of the inferior and lateral temporal lobes, as well as lateral parietal regions. Partial volume correction attenuated the majority of the differences between controls and participants, with both tau-positive and tau-negative cases showing posterior cingulate hypometabolism, and only tau-positive participants showing precuneus and inferior temporal hypometabolism (Supplementary Fig. 1). Direct comparison between tau-positive and tau-negative participants was limited due to the small number of participants, but suggested more medial temporal involvement in tau-negative participants and more inferior temporal involvement in tau-positive participants. The effect size maps revealed large effects in these regions.

Autopsy cohort

Voxel-wise results for the autopsy cohort are shown in Fig. 3. Hippocampal sclerosis participants (most of whom had concomitant Alzheimer's disease) had prominent hypometabolism of the medial temporal lobe, with the inferior and lateral temporal gyri, lateral parietal regions and the posterior cingulate and precuneus involved to a lesser extent. Alzheimer's disease without TDP-43 participants had far less involvement of the medial temporal regions, and had more medial and lateral parietal hypometabolism. Inferior and lateral temporal gyri were involved to a similar extent. Partial volume correction attenuated the majority of the differences between controls and participants, although Alzheimer's disease without TDP-43 participants still had patchy inferior temporal hypometabolism (Supplementary Fig. 1). Direct comparisons were limited due to small numbers, but the medial temporal lobe was significantly more involved in hippocampal sclerosis, whereas medial and lateral parietal regions were significantly more involved in Alzheimer's disease without TDP-43. Large effect sizes were noted in these regions.

Structural imaging findings

Tau-negative and tau-positive participants both had hippocampal atrophy, and all participants fell below the hippocampal volume (HVa) cut-off point of −1.5. Both groups had lower hippocampal volume values than controls, but the tau-positive and tau-negative groups did not differ (Fig. 4A). All participants in the autopsy cohort also had reduced hippocampal volumes (Fig. 5A). Mean hippocampal volume was lower in the hippocampal sclerosis group compared to the Alzheimer's disease group, but not significantly so (Fig. 5A). The ratio of inferior to medial temporal thickness did not differ between tau-positive and tau-negative, or between Alzheimer's disease and hippocampal sclerosis groups (Supplementary Fig. 3).
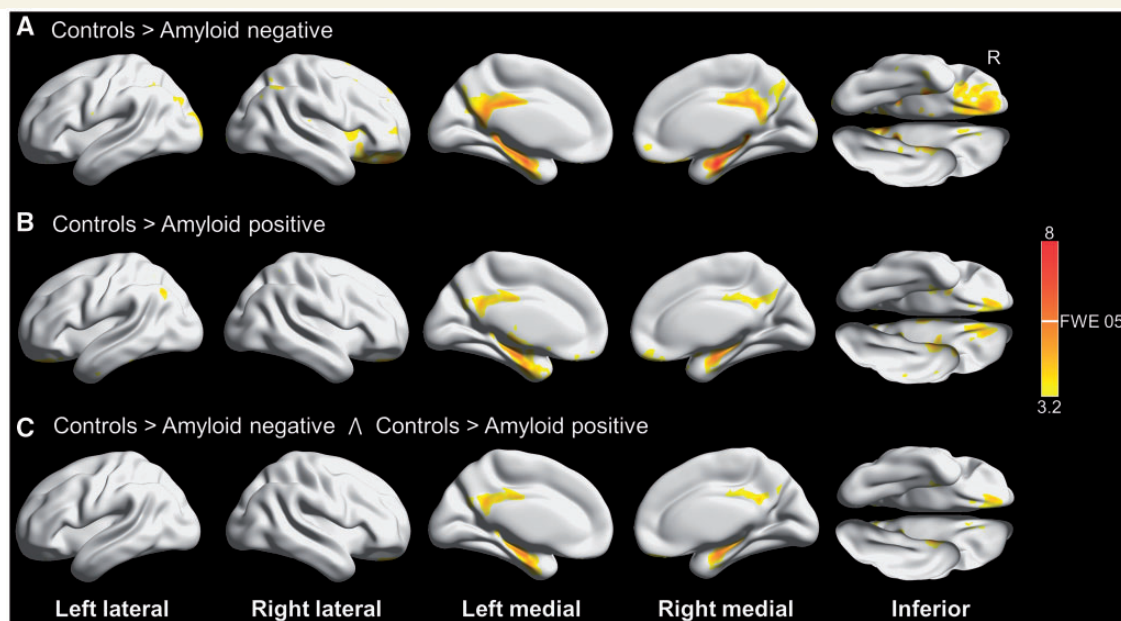
Figure 1 3D brain renderings showing results of FDG-PET analysis in tau-negative patients. Results are shown at *P*(unc) = 0.001 with the height cut-off for family-wise error (FWE) correction shown in the colour bar. (**A**) Compared to controls, tau-negative amyloid-negative participants had hypometabolism in the posterior and middle cingulate and the medial temporal lobes. (**B**) Compared to controls, tau-negative amyloid-positive participants also had hypometabolism in the posterior and middle cingulate and the medial temporal lobes. (**C**) Conjunction analysis of **A** and **B** revealing areas involved in both amyloid-positive and amyloid-negative cases compared to controls. Renders created using Brain Net Viewer (Xia *et al.*, 2013) (https://www.nitrc.org/projects/bnv/).

Region of interest-based FDG-PET

The results of the region of interest-based analysis for tau-positive and tau-negative participants are shown in Fig. 4B. The ratio of inferior to medial temporal metabolism was significantly higher in tau-negative cases compared to controls and tau-positive participants. In addition, this pattern of medial temporal metabolism compared to inferior temporal metabolism was apparent on a single participant level in many cases (Fig. 4C).

Applying the same region of interest analysis to the autopsy cohort yielded comparable results (Fig. 5B). Specifically, the inferior medial/temporal ratio was significantly higher in hippocampal sclerosis cases. The comparison of medial and inferior temporal hypometabolism again appeared helpful on a single participant level (Fig. 5C).

## Imaging and neuropathology findings in tau-negative participants who came to autopsy

As mentioned previously, two tau-negative participants came to autopsy during the study. Both participants presented with a slowly progressive amnestic syndrome, and both were clinically thought to have Alzheimer's disease. The imaging and neuropathological findings in these two index cases are shown in Fig. 6, along with the inferior/medial temporal ratio results from the other participants in the study to provide necessary context. Index Case 1 was amyloid- and tau-negative, whereas index Case 2 was amyloid-positive. Both cases had elevated inferior/medial temporal ratios and focal medial temporal and posterior cingulate hypometabolism on CortexID.

Neuropathological examination in index Case 1 revealed extensive medial temporal and hippocampal sclerosis, with marked neuronal loss and gliosis involving the presubiculum, subiculum, prosubiculum and CA1 regions. There were moderate subicular and hippocampal, and frequent entorhinal, TDP-43 positive dystrophic neurites and neuronal cytoplasmic inclusions. NIA-AA staging of Alzheimer's disease pathological change was A1B1C1 (low). Tau pretangles and neurites were noted in the subiculum. Frequent medial temporal silver-positive and 4R-tau-immunoreactive grains were noted, along with coiled bodies in the temporal lobe and pretangles in the amygdala, consistent with argyrophillic grain disease.

Neuropathological examination in index Case 2 revealed an intermediate degree of Alzheimer's disease neuropathologic change (A2B2C2), with moderate-to-frequent diffuse and neuritic plaques within the mesial temporal structures and moderate plaque burden in the neocortex, frequent neurofibrillary tangles and ghost tangles in the mesial temporal lobe and sparse tangles in the neocortex. Severe neuronal loss and gliosis involving primarily the CA1 and CA2 regions of the hippocampus, and to a lesser extent the amygdala and entorhinal cortex were noted, consistent
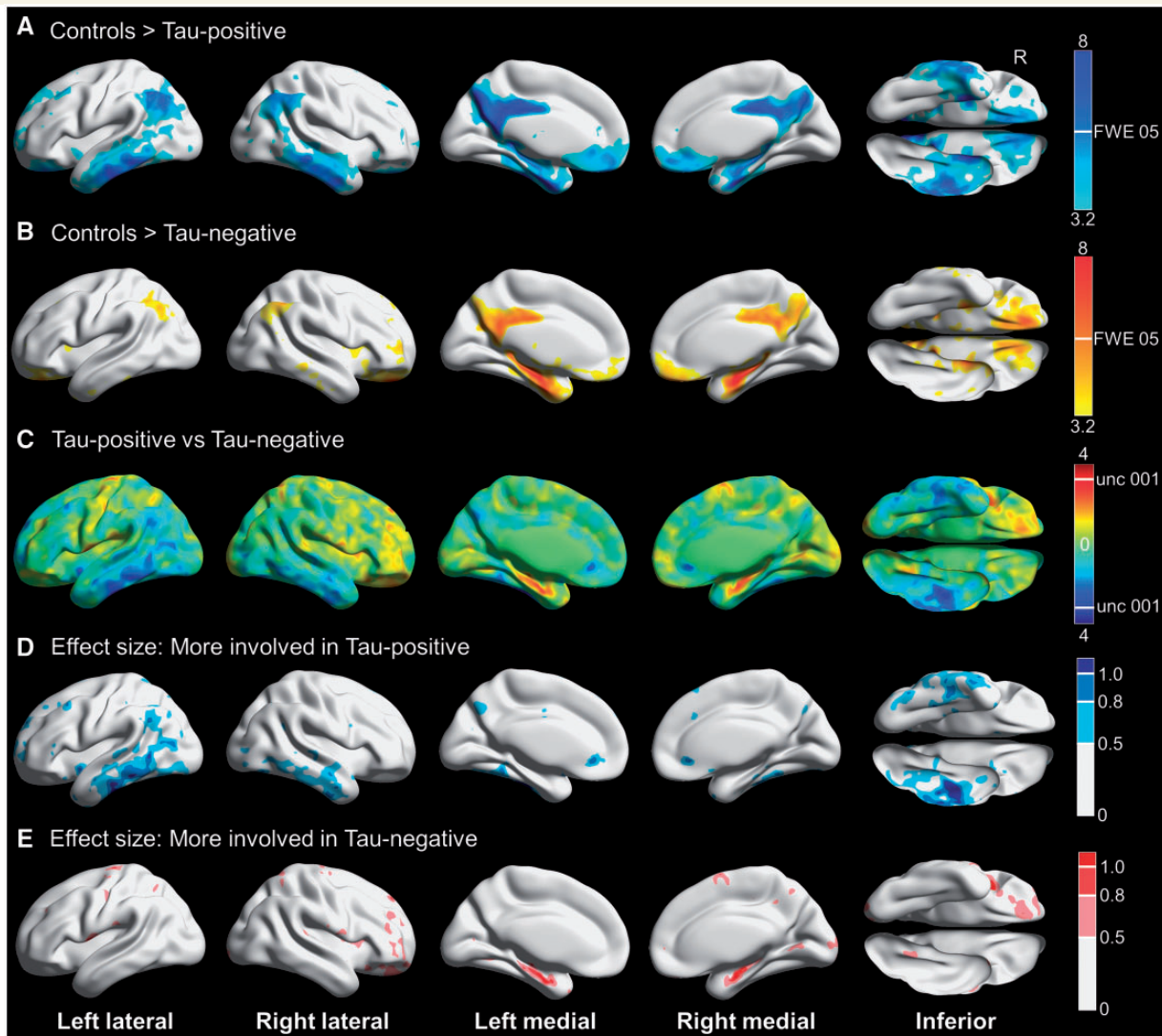
Figure 2 Three-dimensional brain renderings showing results of FDG-PET analysis in tau-negative and tau-positive participants. Compared to controls, tau-positive participants also had hypometabolism in the posterior and middle cingulate and the precuneus, but there was more widespread cortical involvement including inferior and middle temporal gyri and the angular gyri bilaterally. In addition, medial temporal lobe involvement was less pronounced. Results are shown at P(unc) = 0.001 with the height cut-off for FWE correction shown in the colour bar. (**B**) Compared to controls, tau-negative participants had hypometabolism in the posterior and middle cingulate, the inferior precuneus and the medial temporal lobe. Results are shown at P(unc) = 0.001 with the height cut-off for family-wise error (FWE) correction shown in the colour bar. (**C**) T-map for tau-negative compared to tau-positive participants, with red-yellow indicating regions more involved in tau-negative participants and blue-cyan showing areas more involved in tau-positive participants. Although very few voxels are above the height cut-off for P(unc) = 0.001, the medial temporal lobe appears to be more involved in tau-negative cases while the inferior temporal gyri appear more involved in tau-positive cases. (**D**) Effect size (Cohen's d) maps for the direct comparison showing areas of greater involvement in tau-positive cases, including moderate (0.5–0.8) to large ($>$0.8) effect sizes in the inferior temporal gyri. (**E**) Effect size (Cohen's d) maps for the direct comparison showing areas of greater involvement in tau-negative cases, revealing moderate (0.5–0.8) to large ($>$0.8) effect sizes for the medial temporal lobe. Renders created using Brain Net Viewer (Xia *et al.*, 2013) (https://www.nitrc.org/projects/bnv/).

with a diagnosis of hippocampal sclerosis. Frequent TDP-43 positive inclusions and neurites were noted. In addition, there was evidence for cerebral amyloid angiopathy, primarily involving the occipital lobe, and limbic/transitional Lewy body disease. None of the tau-positive participants came to autopsy during the study.

Discussion

In the present study we assessed the utility of FDG-PET for identifying cases where non-Alzheimer's pathology underlies, or contributes to, amnestic MCI or dementia in elderly participants. Our major findings include: (i) cases of tau
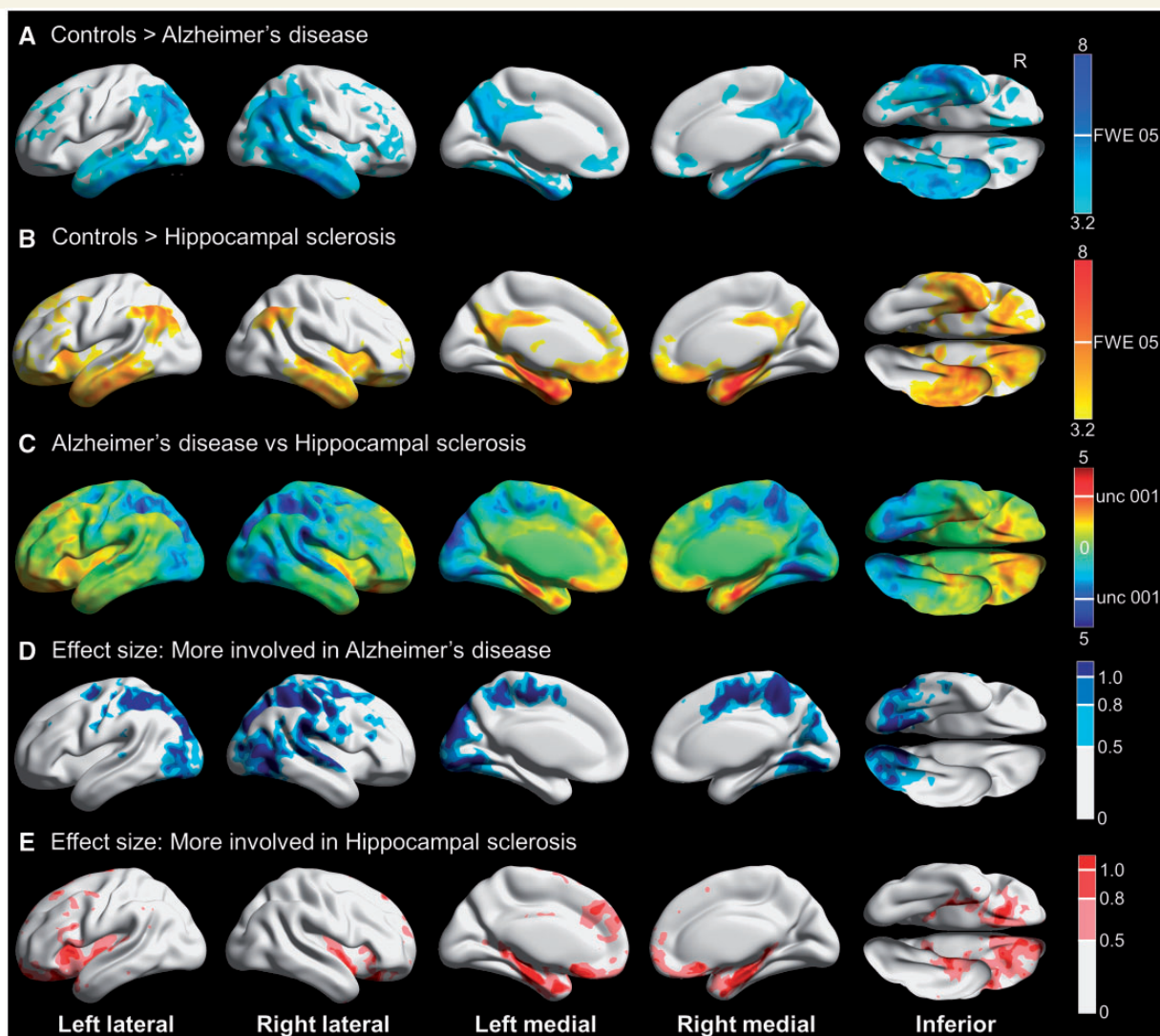
Figure 3 3D brain renderings showing results of FDG-PET analysis in hippocampal sclerosis and Alzheimer's disease participants. (**A**) Compared to controls, TDP-43 negative Alzheimer's disease was associated with hypometabolism of the posterior cingulate, middle and inferior temporal and lateral and medial parietal regions including the precuneus. There was minimal medial temporal involvement. Results are shown at P(unc) = 0.001 with the height cut-off for FWE correction shown in the colour bar. (**B**) Compared to controls, TDP-43-positive hippocampal sclerosis was associated with hypometabolism predominantly in the medial temporal lobe, with additional involvement of the middle and inferior temporal, lateral parietal and insular regions. Results are shown at P(unc) = 0.001 with the height cut-off for family-wise error (FWE) correction shown in the colour bar. Note that most hippocampal sclerosis cases had concomitant Alzheimer's disease. (**C**) T-map for hippocampal sclerosis compared to Alzheimer's disease, with red-yellow indicating regions more involved in hippocampal sclerosis and blue-cyan showing areas more involved in Alzheimer's disease. There was more medial temporal and orbitofrontal involvement in hippocampal sclerosis, and more posterior-inferior temporal, occipital and parietal involvement in Alzheimer's disease. (**D**) Effect size (Cohen's d) map for the direct comparison showing areas of greater involvement in Alzheimer's disease, including moderate (0.5–0.8) to large (>0.8) effect sizes for the posterior-inferior temporal, occipital and parietal regions. (**E**) Effect size (Cohen's d) map for the direct comparison showing areas of greater involvement in hippocampal sclerosis, including moderate (0.5–0.8) to large (>0.8) effect sizes for the medial temporal and orbitofrontal regions. Renders created using Brain Net Viewer (Xia *et al.*, 2013) (https://www.nitrc.org/projects/bnv/).

negative amnestic MCI and dementia (i.e. non Alzheimer's disease) did not differ significantly on neuropsychological testing or measures of hippocampal volume when compared to tau positive (i.e. Alzheimer's disease) cases; (ii) tau-negative amnestic MCI and dementia was associated with focal medial temporal and posterior cingulate hypometabolism regardless of amyloid status; (iii) this pattern of predominantly medial temporal hypometabolism resembled the pattern of hypometabolism seen in autopsy proven TDP-43 positive hippocampal sclerosis; and (iv) a higher
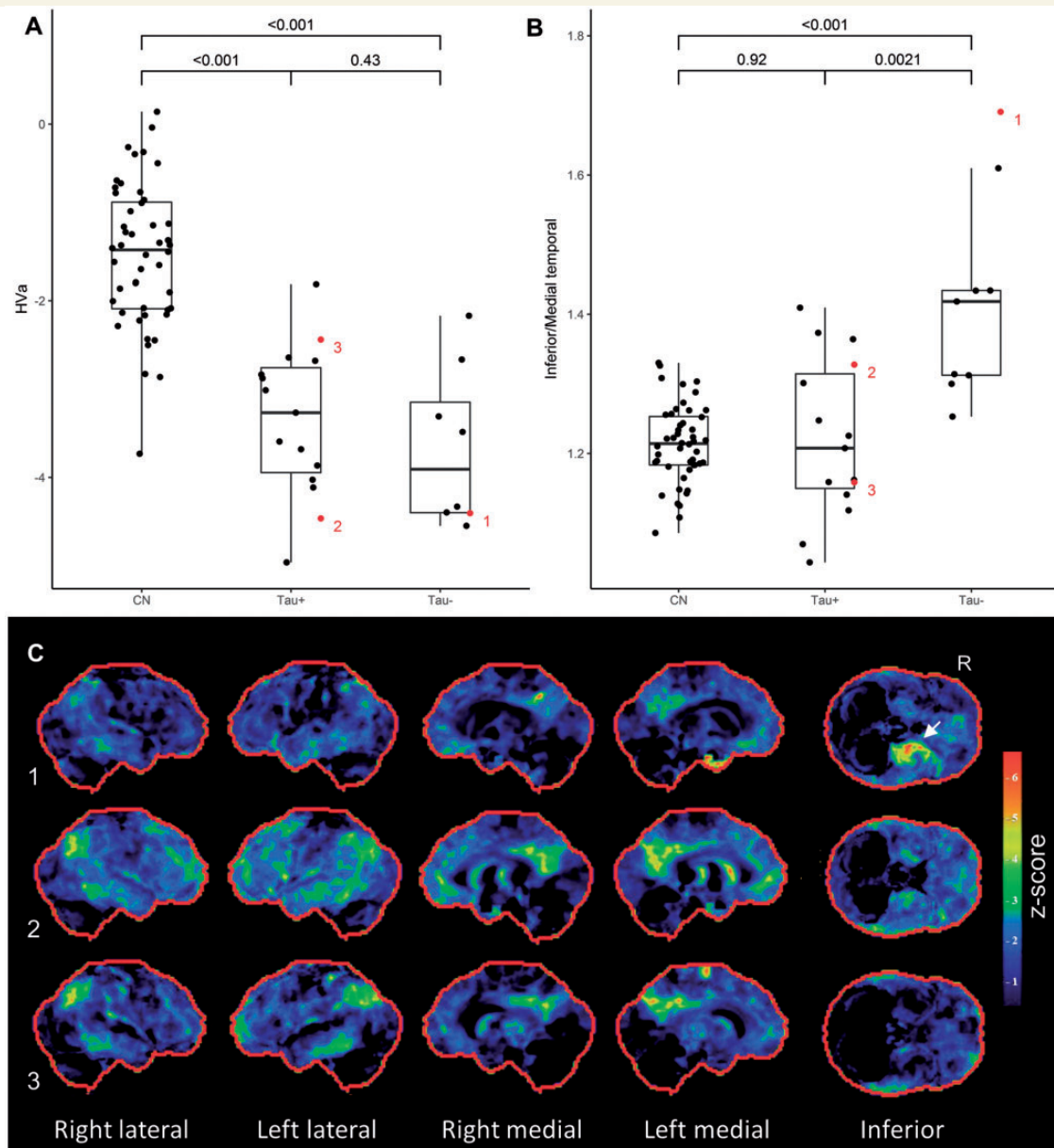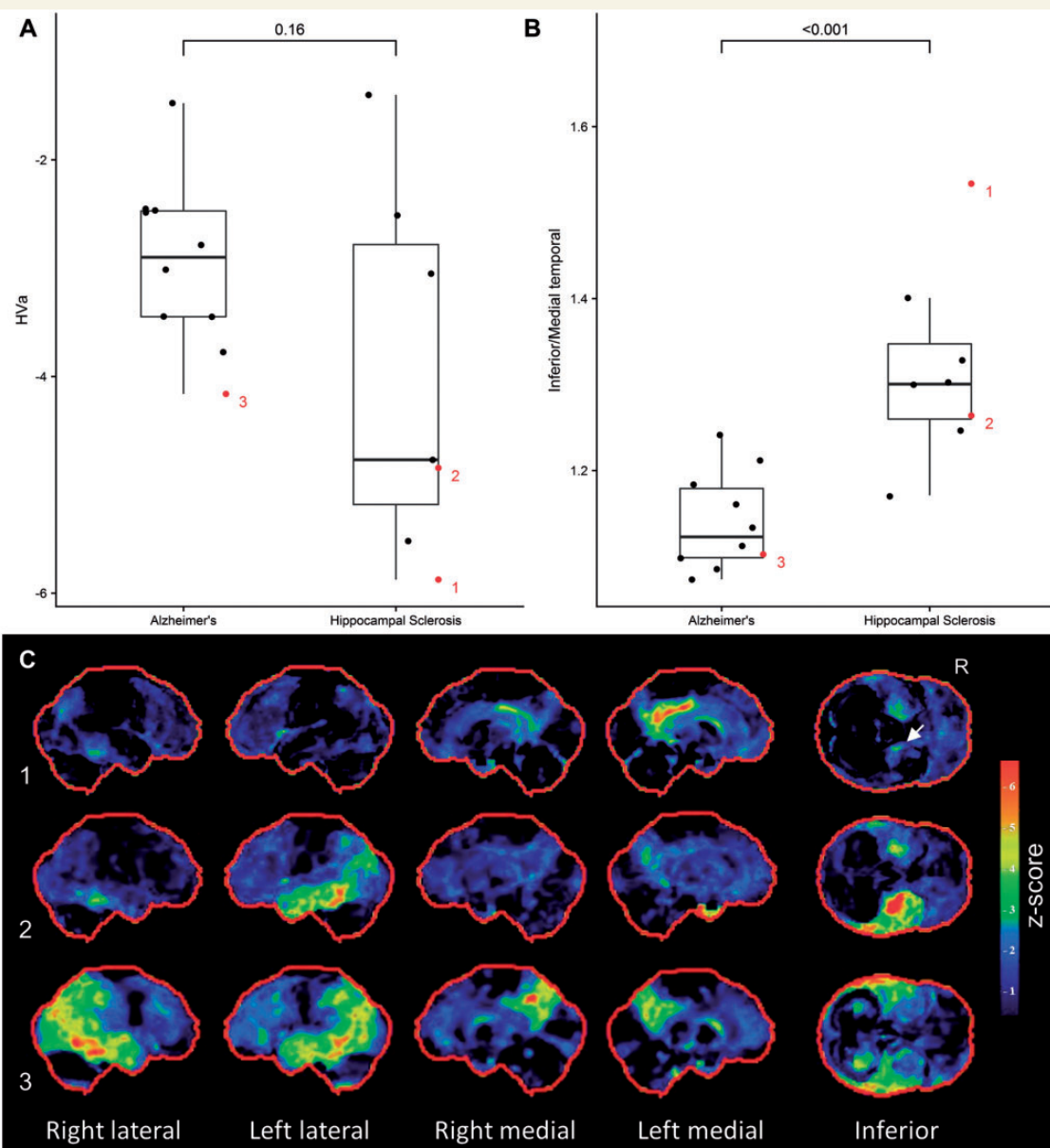
Figure 4 Quantitative imaging findings and examples of participant level FDG-PET scans for the clinical cohort. (A) Both tau-positive and tau-negative participants had reduced adjusted hippocampal volumes (HVa) compared to controls, but were not significantly different from one another. **(B)** The ratio of inferior temporal metabolism over medial temporal metabolism was significantly higher in tau-negative participants compared to controls and tau-positive participants. **(C)** Examples of participant level FDG-PET statistical stereotactic surface projection maps generated by Cortex ID (GE Healthcare) for three participants. Numbers 1–3 refer to the labels in **B**. Note the disproportionate medial temporal hypometabolism in 1 (A + /T−), the relative sparing of medial temporal structures in 3 (A + /T +) and the overlapping pattern in 2 (A + /T +), with a corresponding intermediate inferior/medial temporal ratio. CN = cognitively normal.

ratio of inferior to medial temporal metabolism differentiated tau-positive from tau-negative cases as well as autopsy-confirmed TDP-43 positive hippocampal sclerosis from TDP-43 negative Alzheimer's disease and also accurately predicted the presence of this pathology in two of two subjects from the clinical cohort that came to autopsy during this study. We discuss the implications of these results below.

Neuropsychological performance and hippocampal volume do not differentiate tau-positive and negative dementia

There were no clear differences on neuropsychological testing or structural imaging between tau-positive and

Figure 5 Quantitative imaging findings and examples of participant level PET scans for the autopsy cohort. (**A**) There was a trend towards smaller hippocampal volume in hippocampus sclerosis, although this did not reach statistical significance. (**B**) The ratio of inferior temporal metabolism over medial temporal metabolism was significantly higher in hippocampal sclerosis cases compared Alzheimer's disease. (**C**) Examples of participant level FDG-PET statistical stereotactic surface projection maps generated by Cortex ID (GE Healthcare) for three participants. Numbers 1–3 refer to the labels in **B**. Note the focal medial temporal and posterior cingulate hypometabolism in 1 (hippocampal sclerosis with Alzheimer's disease, A5B5C2, PET completed 4 years before death), the relative sparing of medial temporal structures in 3 (Alzheimer's disease without hippocampal sclerosis, A4B6C2, PET completed 4 years before death) and the overlapping pattern in 2 (hippocampal sclerosis with Alzheimer's disease, A3B5C2, PET completed 4 years before death).

tau-negative cases, implying that the tau-negative group mimics Alzheimer's disease closely. Our results suggest that, while this issue may be rare below the age of 75, approximately a third of patients with an amnestic presentation above that age may in fact be tau-negative. This is in keeping with previous work that has shown a 10-fold increase in the number of suspected non-amyloid pathology

patients between ages 65–85 (Jack *et al.*, 2016b) and with more recent population-based studies using flortaucipir (Jack *et al.*, 2017). The findings here emphasize the importance of considering amyloid and tau separately when defining Alzheimer's disease from a molecular perspective, in keeping with the NIA-AA research framework (Dubois *et al.*, 2016). That is to say, by using a classification such
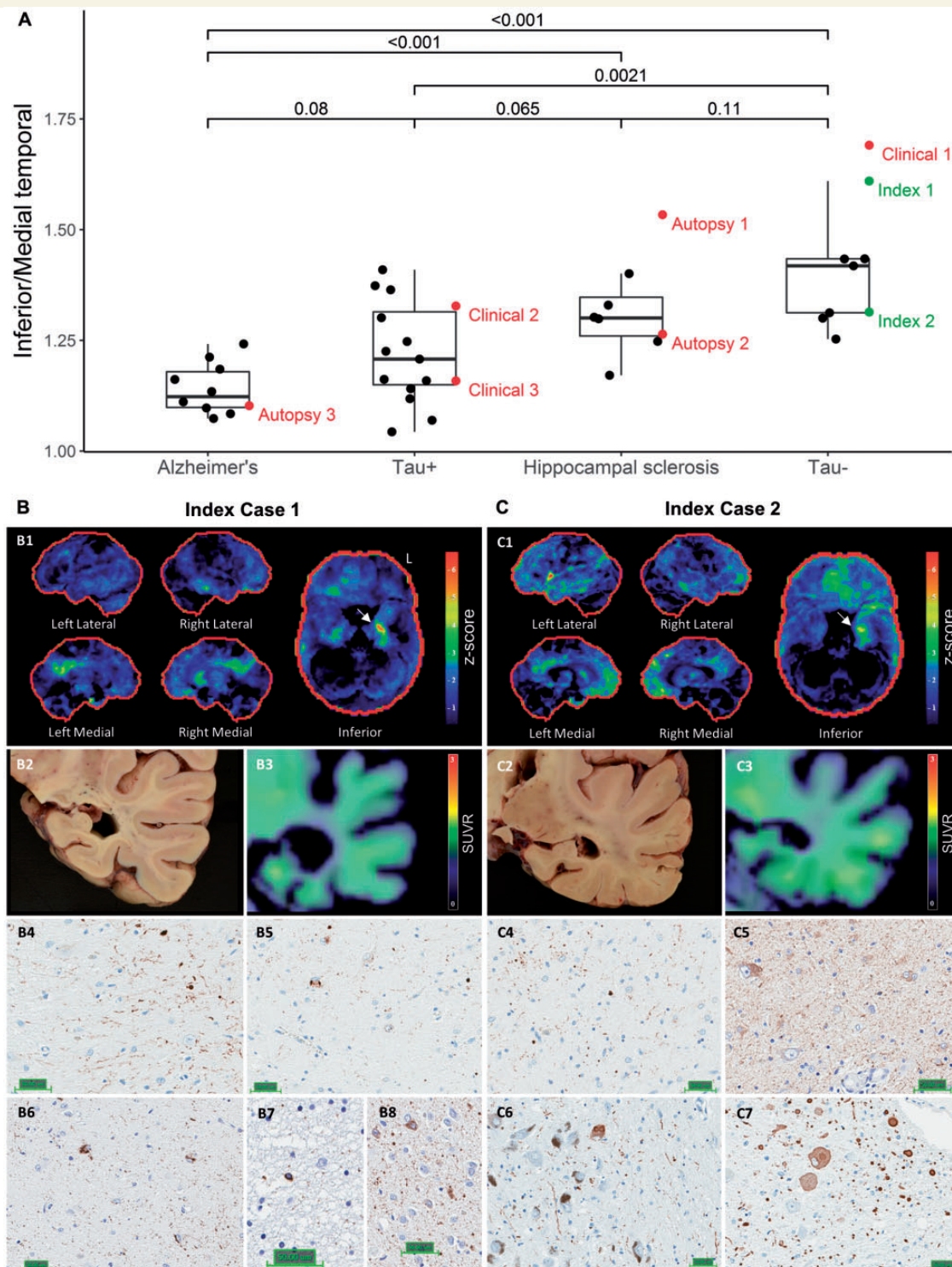
Figure 6 **Imaging and neuropathology findings in the two index tau-negative cases that came to autopsy during the study.**
(**A**) The ratio of inferior/medial temporal metabolism is shown for both the clinical and autopsy cohorts, with the same three cases highlighted as in Fig. 4 (Clinical 1–3) and Fig. 5 (Autopsy 1–3) in red. The two index cases are highlighted in green. (**B**) Participant level results for index Case 1. The participant's FDG-PET (Cortex ID) is shown in **B1**, illustrating medial temporal and posterior cingulate hypometabolism with sparing of inferior temporal and lateral parietal regions. A gross pathological image at the level at which the hippocampal biopsies were taken is shown in **B2**, and flortaucipir PET at the same level is shown in **B3**. Results of immunohistochemical staining of hippocampal sections for TDP-43 are shown in **B4–5** (Scale bar = 50 μm), which revealed dystrophic neurites (**B4**) and neuronal cytoplasmic inclusions (**B5**). Results of tau immunostaining are presented in **B6–8** (Scale bar = 50 μm), showing pretangles in the subiculum (**B6**), a coiled body in the temporal lobe (**B7**) as well as pretangles and grains in the amygdala (**B8**). (**C**) Participant level results for index Case 2. As can be seen in **C1**, this participant had predominantly left medial temporal and orbitofrontal hypometabolism on FDG-PET (Cortex ID). There was more involvement of the inferior temporal and lateral parietal

(continued)

at the A/T/N framework, clinically impaired A + /T−/N + participants are identified appropriately as distinct from T + participants. This has implication for clinical trial design in that such participants may benefit less, or not at all, from therapeutic agents targeting Alzheimer's disease pathology such as amyloid and tau since they likely harbour concomitant non-Alzheimer's pathology. This is evidently not as pertinent for clinically unimpaired patients, a group where the therapeutic focus may be amyloidosis in the absence of tau.

FDG-PET in tau-negative amnestic dementia resembles that of autopsy-proven hippocampal sclerosis

A previous study reported relatively restricted posterior cingulate and retrosplenial hypometabolism in amyloid-negative cases clinically diagnosed with typical Alzheimer's disease dementia, which contrasted with the more widespread hypometabolism seen in amyloid-positive cases (Chetelat *et al.*, 2016). We found a similar pattern of hypometabolism in all tau-negative cases, regardless of amyloid status, in contrast to tau-positive cases who had more widespread association cortex involvement, especially in inferior and lateral temporal regions, regions typically associated with Alzheimer's disease. On direct comparison of tau-negative and tau-positive participants, the largest effect was seen in medial and inferior temporal regions.

Because isocortical tau PET abnormalities are tightly linked to overt cognitive impairment (Jack *et al.*, 2013; Pontecorvo *et al.*, 2017), subjects with elevated amyloid but who lack elevated tau probably harbour additional pathology explaining the majority of their cognitive impairment. The FDG pattern described here may be helpful in identifying non-Alzheimer's pathology in the setting of amnestic cognitive disorders, either as co-pathology (in those that are amyloid-positive, for example) or as primary pathology. In other words, in a patient above the age of 75 with an amnestic syndrome and FDG-PET hypometabolism restricted to the medial temporal lobe and posterior cingulate cortex, non-Alzheimer's degenerative aetiologies should be suspected.

We hypothesized that hippocampal sclerosis accounted for a significant proportion of tau-negative amnestic dementia cases and tested this by performing the same PET analysis in an autopsy-proven cohort of TDP-43-positive hippocampal sclerosis and TDP-43-negative Alzheimer's disease participants. When compared to controls, the

Alzheimer's group as expected resembled the tau-positive cohort, with medial and lateral parietal, lateral and inferior temporal and occipital hypometabolism bilaterally. Results in the hippocampal sclerosis group resembled a mix between the tau-negative and tau-positive groups. Similar to the tau-negative group, the hippocampal sclerosis group had the most severe hypometabolism in the medial temporal lobe. However, the latter group had more pronounced involvement of the inferior and lateral temporal lobes and the lateral parietal lobes. This likely reflects the fact that most of our hippocampal sclerosis participants had co-existing Alzheimer's disease (i.e. they would probably have been classified as tau-positive), consistent with prior reports that hippocampal sclerosis in the absence of Alzheimer's pathology is rare (Zarow *et al.*, 2008; Dawe *et al.*, 2011). On direct comparison, the regions that were more involved in hippocampal sclerosis compared to Alzheimer's disease were similar to those that were more involved in tau-negative compared to tau-positive cases, supporting our hypothesis. However, other limbic predominant neurodegenerative processes, such as argyrophilic grain disease, may also contribute to this finding.

The inferior to medial temporal metabolism ratio separates amnestic mimics from Alzheimer's disease

Although the direct comparison between tau-positive and tau-negative cases did not reach statistical significance, at the voxel level there were regions of large effect size in the inferior and medial temporal lobes. As mentioned previously, we quantified this pattern in a region of interest-based analysis. There is an obvious circularity here, in that the regions of peak effect size differentiating tau-positive and tau-negative cases were used as a basis for region of interest selection. As such, the fact that the inferior/medial temporal ratio differentiates these groups is not surprising. However, we should emphasize that we took regions of interest from a widely used atlas in order to simplify replication, and used regions that were far larger than the areas of peak effect size. In addition, this exercise was far from futile in that it allowed for the quantification of the aforementioned pattern at a single participant level, a crucial requirement for any potential biomarker.

We applied this same region of interest analysis to the autopsy cohort, and showed that the inferior/medial tem-

Figure 6 Continued

regions than in index Case 1. A gross pathological image at the level at which the hippocampal biopsies were taken is shown in **C2**, and flortaucipir PET at the same level is shown in **C3**. Although this participant was also below the flortaucipir cut-off point, there appeared to be a greater degree of low-level binding than in index Case 1. Immunohistochemical staining for TDP-43 showing dystrophic neurites presented in **C4** (Scale bar = 50 μm). A tau immunostain showing pretangles is presented in **C5** (Scale bar = 50 μm). Alpha-synuclein immunohistochemistry results are presented in **C6–7** (Scale bar = 50 μm), demonstrating Lewy bodies in the midbrain (**C6**) and medulla (**C7**).

poral ratio was significantly elevated in hippocampal sclerosis participants compared to Alzheimer's disease participants. We would like to emphasize that, in the autopsy cohort, the caveats about circularity mentioned previously do not apply. Our results suggest that the ratio of inferior temporal to medial temporal metabolism among elderly participants with an amnestic syndrome may serve to not only identify tau-negative cases, but could point towards hippocampal sclerosis as an underlying pathology.

In many cases the patterns described at group level were evident on the participant level PET scans, such as the restricted medial temporal and posterior cingulate hypometabolism in the tau-negative participant shown in Fig. 4C, or involvement of the inferior temporal gyrus with relative sparing of the medial temporal lobe in the TDP-43 negative Alzheimer's disease patient shown in Fig. 5C. In some participants the posterior cingulate hypometabolism was more apparent than the medial temporal hypometabolism [e.g. in Fig. 5C(1)], and it may be that hypometabolism restricted to the posterior cingulate cortex (inverse cingulate island sign) can serve as additional evidence for hippocampal sclerosis. The single participant level utility can also be seen in the two tau-negative cases that came to autopsy during the study, who both had elevated inferior/medial temporal ratios and evidence for the tau-negative/hippocampal sclerosis pattern on Cortex ID.

FDG-PET has the potential to identify cases of mixed hippocampal sclerosis and Alzheimer's disease

A central issue in the study of degenerative disease in the elderly is identifying multiple co-occurring pathologies during life. This is important for clinical trial design, where one would ideally recruit patients that have the pathological substrate you are targeting and do not have additional pathologies that may dampen or mask a clinical benefit from the therapeutic agent. Our focus here has been on using FDG-PET to discern tau-positive versus tau-negative amnestic dementia, and hippocampal sclerosis versus Alzheimer's disease, but it is worth remembering that there is a plethora of other pathologies that may contribute to cognitive decline. Nevertheless, the data reported here suggest a potential role for FDG-PET in identifying multiple co-occurring pathologies during life.

This is best illustrated by Fig. 6, where the tau negative case with the higher inferior/medial temporal ratio had a low stage of Alzheimer's disease pathological change at autopsy, whereas the case with a lower ratio had an intermediate stage. This latter case fell in the range of the hippocampal sclerosis cases from the autopsy cohort, most of whom also had co-existing Alzheimer's disease. Figure 6 also illustrates the complexity of trying to sort out multiple pathologies in this cohort. Specifically, the Alzheimer's disease group was 'pure' in the sense that there was no evidence for hippocampal sclerosis and TDP-43 staining was negative. Similarly, it is unlikely that Alzheimer's disease is the primary driver of neurodegeneration and clinical symptoms in the tau-negative group. That is to say, even though some of these participants were amyloid-positive, such as index Case 2, and it is possible that some harbour low Braak stage of neurofibrillary pathology, there would have to be a non-Alzheimer's pathology to account for the significant atrophy and cognitive impairment in the absence of significant flortaucipir binding. In contrast, the tau-positive and hippocampal sclerosis groups fall somewhere in-between, and overlap substantially. The fact that most of the hippocampal sclerosis participants had co-existing Alzheimer's disease explains the intermediate ratio in that group. Some of the tau-positive cases had relatively elevated ratios, and we postulate that these cases harbour hippocampal sclerosis in addition to Alzheimer's pathology. Alternatively, the elevated ratio could be due to any number of pathologies affecting the hippocampus, including medial temporal involvement from Alzheimer's disease itself.

There are two important aspects of Alzheimer's disease and hippocampal sclerosis co-pathology we did not address. The first concerns the role of TDP-43 in the absence of the pathological stigmata of hippocampal sclerosis. The second pertains to TDP-43 associated hippocampal sclerosis in the setting of frontotemporal dementia, i.e. not hippocampal sclerosis of ageing.

The relationship between TDP-43, hippocampal sclerosis and Alzheimer's pathology is a matter of ongoing debate. In the autopsy cohort, we limited our hippocampal sclerosis participants to those who were TDP-43 positive in order to identify those participants who likely had a degenerative basis for their hippocampal sclerosis. Prior reports suggest ~90% of cases are TDP-43 positive, provided the anterior hippocampus and amygdala are screened (Zarow *et al.*, 2008; Nelson *et al.*, 2011; Pao *et al.*, 2011). Similarly, we chose to limit our Alzheimer's cohort to those that were TDP-43 negative. TDP-43-positive inclusions frequently occur in Alzheimer's disease and are often not associated with the stigmata of hippocampal sclerosis (Josephs *et al.*, 2014). Even in the absence of neuronal loss suggestive of hippocampal sclerosis, the presence of TDP-43 inclusions in Alzheimer's disease is associated with worse performance on memory testing and smaller hippocampal volumes (Josephs *et al.*, 2014). However, it is common practice to only examine one hemisphere, despite the fact that hippocampal sclerosis is often unilateral (Zarow *et al.*, 2008, 2012; Nelson *et al.*, 2011). In unilateral cases, TDP-43 is still found bilaterally, and it is possible that some TDP-43-positive but hippocampal sclerosis-negative cases did, in fact, have unilateral sclerosis. Alternatively, it may be that some participants have the neuropathological substrate of TDP-43 but are yet to develop the focal neuronal loss. In younger participants, non-age-related hippocampal sclerosis and alternative degenerative disorders associated with TDP-43, such as frontotemporal dementia and

semantic dementia, further complicates the relationship between TDP-43 and Alzheimer's disease.

By limiting our analysis to those ⩾75 years of age, and focusing on TDP-43-negative Alzheimer's disease and TDP-43-positive hippocampal sclerosis, many of these issues were avoided, perhaps at the expense of generalizability. Recent evidence suggests that hippocampal sclerosis seen in association with advanced age is distinct from that seen in younger patients or in association with frontotemporal dementia (Cykowski *et al.*, 2017), and future studies will have to examine the potential for FDG-PET to identify hippocampal sclerosis in younger participants and test the utility of the ratio described here in TDP-43 positive Alzheimer's disease.

Limitations

As we have pointed out previously, there are several important limitations to the current study. First, the relatively small numbers in each group limited our statistical power. This is a common problem in this area of research, and prior studies elected not to directly compare diseased groups (Chetelat *et al.*, 2016). Despite not reaching statistical significance, we had large effect sizes and supplemented our findings with a region of interest-based analysis, which was highly significant. While there was circularity with the region of interest-based analyses being informed by the voxel-wise results, we were able to independently demonstrate a significant region of interest-based result in the autopsy cohort. As this is a first attempt at *in vivo* FDG-based markers of hippocampal sclerosis, we also selected relatively 'pure' cases for our autopsy cohort, which limits the generalizability. Future studies will have to address the question of TDP-43 in the absence of hippocampal sclerosis, cases of Alzheimer's disease and hippocampal sclerosis mixed with other pathologies such as dementia with Lewy Bodies and cases below the age of 75. Since our patients were all seen at the Alzheimer's Disease Research Center or Mayo Clinic Study of Aging, associated with a single tertiary care centre, there is likely some degree of selection bias present. Finally, although the meta-region of interest used to classify participants as tau-positive or tau-negative was designed without considering a particular Alzheimer's disease dementia phenotype, it is possible that it would be less sensitive in atypical phenotypes. Since we were primarily interested in the typical, amnestic phenotype in the present study and visually reviewed all tau PET images it is unlikely that any atypical Alzheimer's disease dementia cases were included in the tau-negative group.

Conclusions

In conclusion, we have shown that tau-negative amnestic dementia in those older than 75 is associated with a signature pattern of hypometabolism regardless of amyloid status. This pattern, with medial greater than inferior temporal hypometabolism associated with posterior cingulate hypometabolism and sparing of the lateral association cortices, is shared by cases of hippocampal sclerosis. We have also proposed the ratio of inferior to medial temporal metabolism as a way of quantifying this, which was able to differentiate tau-positive from tau-negative cases, and cases of hippocampal sclerosis from TDP-43-negative Alzheimer's disease. We propose that a pattern of medial temporal hypometabolism out of proportion to inferior temporal hypometabolism serve as an antemortem marker of TDP-43 associated hippocampal sclerosis of ageing. This is a testable hypothesis, and clearly preliminary at this stage. It is unclear how specific these findings are for hippocampal sclerosis as opposed to any limbic predominant pathology (limbic predominant Alzheimer's disease, argyrophilic grain disease), or indeed what would happen if more mixed cases are included (dementia with Lewy bodies co-existing with Alzheimer's disease, or TDP-43 positive Alzheimer's disease without hippocampal sclerosis). We are planning to address these questions in future studies.

Acknowledgements

Funding

Supplementary material

Supplementary material is available at *Brain* online.

References

Albert MS, DeKosky ST, Dickson D, Dubois B, Feldman HH, Fox NC, et al. The diagnosis of mild cognitive impairment due to Alzheimer's disease: recommendations from the National Institute on Aging-Alzheimer's Association workgroups on diagnostic guidelines for Alzheimer's disease. Alzheimers Dement 2011; 7: 270–9.

Barret O, Alagille D, Sanabria S, Comley RA, Weimer RM, Borroni E, et al. Kinetic modeling of the Tau PET tracer (18)F-AV-1451 in human healthy volunteers and Alzheimer disease subjects. J Nucl Med 2017; 58: 1124–31.

Chetelat G, Ossenkoppele R, Villemagne VL, Perrotin A, Landeau B, Mezenge F, et al. Atrophy, hypometabolism and clinical trajectories in patients with amyloid-negative Alzheimer's disease. Brain 2016; 139: 2528–39.

Cykowski MD, Powell SZ, Schulz PE, Takei H, Rivera AL, Jackson RE, et al. Hippocampal sclerosis in older patients practical examples and guidance with a focus on cerebral age-related TDP-43 with sclerosis. Arch Pathol Lab Med 2017; 141: 1113–26.

Dawe RJ, Bennett DA, Schneider JA, Arfanakis K. Neuropathologic correlates of hippocampal atrophy in the elderly: a clinical, pathologic, postmortem MRI study. PLoS One 2011; 6: e26286.

Dickson DW, Davies P, Bevona C, Van Hoeven KH, Factor SM, Grober E, et al. Hippocampal sclerosis: a common pathological feature of dementia in very old (> or = 80 years of age) humans. Acta Neuropathol 1994; 88: 212–21.

Dubois B, Hampel H, Feldman HH, Scheltens P, Aisen P, Andrieu S, et al. Preclinical Alzheimer's disease: definition, natural history, and diagnostic criteria. Alzheimers Dement 2016; 12: 292–323.

Fischl B, Salat DH, Busa E, Albert M, Dieterich M, Haselgrove C, et al. Whole brain segmentation: automated labeling of neuroanatomical structures in the human brain. Neuron 2002; 33: 341–55.

Fischl B, Salat DH, van der Kouwe AJ, Makris N, Segonne F, Quinn BT, et al. Sequence-independent segmentation of magnetic resonance images. Neuroimage 2004; 23: S69–84.

Gorno-Tempini ML, Dronkers NF, Rankin KP, Ogar JM, Phengrasamy L, Rosen HJ, et al. Cognition and anatomy in three variants of primary progressive aphasia. Ann Neurol 2004; 55: 335–46.

Greve DN, Salat DH, Bowen SL, Izquierdo-Garcia D, Schultz AP, Catana C, et al. Different partial volume correction methods lead to different conclusions: an F-18-FDG-PET study of aging. Neuroimage 2016; 132: 334–43.

Han X, Fischl B. Atlas renormalization for improved brain MR image segmentation across scanner platforms. IEEE T Med Imaging 2007; 26: 479–86.

Hyman BT, Phelps CH, Beach TG, Bigio EH, Cairns NJ, Carrillo MC, et al. National Institute on Aging-Alzheimer's Association guidelines for the neuropathologic assessment of Alzheimer's disease. Alzheimers Dement 2012; 8: 1–13.

Jack CR, Bennett DA, Blennow K, Carrillo MC, Feldman HH, Frisoni GB, et al. A/T/N: an unbiased descriptive classification scheme for Alzheimer disease biomarkers. Neurology 2016a; 87: 539–47.

Jack CR, Knopman DS, Jagust WJ, Petersen RC, Weiner MW, Aisen PS, et al. Tracking pathophysiological processes in Alzheimer's disease: an updated hypothetical model of dynamic biomarkers. Lancet Neurol 2013; 12: 207–16.

Jack CR, Knopman DS, Weigand SD, Wiste HJ, Vemuri P, Lowe V, et al. An operational approach to National Institute on Aging-Alzheimer's Association criteria for preclinical Alzheimer disease. Ann Neurol 2012; 71: 765–75.

Jack CR, Therneau TM, Wiste HJ, Weigand SD, Knopman DS, Lowe VJ, et al. Transition rates between amyloid and neurodegeneration biomarker states and to dementia: a population-based, longitudinal cohort study. Lancet Neurol 2016b; 15: 56–64.

Jack CR, Wiste HJ, Weigand SD, Therneau TM, Lowe VJ, Knopman DS, et al. Defining imaging biomarker cut points for brain aging and Alzheimer's disease. Alzheimers Dement 2017; 13: 205–16.

Josephs KA, Whitwell JL, Weigand SD, Murray ME, Tosakulwong N, Liesinger AM, et al. TDP-43 is a key player in the clinical features associated with Alzheimer's disease. Acta Neuropathol 2014; 127: 911–24.

McKeith IG, Boeve BF, Dickson DW, Halliday G, Taylor JP, Weintraub D, et al. Diagnosis and management of dementia with Lewy bodies Fourth consensus report of the DLB Consortium. Neurology 2017; 89: 88–100.

McKhann GM, Knopman DS, Chertkow H, Hyman BT, Jack CR, Kawas CH, et al. The diagnosis of dementia due to Alzheimer's disease: recommendations from the National Institute on Aging-Alzheimer's Association workgroups on diagnostic guidelines for Alzheimer's disease. Alzheimers Dement 2011; 7: 263–9.

Meltzer CC, Kinahan PE, Greer PJ, Nichols TE, Comtat C, Cantwell MN, et al. Comparative evaluation of MR-based partial-volume correction schemes for PET. J Nucl Med 1999; 40: 2053–65.

Mirra SS, Heyman A, McKeel D, Sumi SM, Crain BJ, Brownlee LM, et al. The Consortium to Establish a Registry for Alzheimer's Disease (CERAD). Part II. Standardization of the neuropathologic assessment of Alzheimer's disease. Neurology 1991; 41: 479–86.

Mishra S, Gordon BA, Su Y, Christensen J, Friedrichsen K, Jackson K, et al. AV-1451 PET imaging of tau pathology in preclinical Alzheimer disease: defining a summary measure. Neuroimage 2017; 161: 171–8.

Monsell SE, Dodge HH, Zhou XH, Bu YQ, Besser LM, Mock C, et al. Results From the NACC uniform data set neuropsychological battery crosswalk study. Alzheimer Dis Assoc Disord 2016; 30: 134–9.

Mortimer JA. The Nun Study: risk factors for pathology and clinical-pathologic correlations. Curr Alzheimer Res 2012; 9: 621–7.

Murray ME, Cannon A, Graff-Radford NR, Liesinger AM, Rutherford NJ, Ross OA, et al. Differential clinicopathologic and genetic features of late-onset amnestic dementias. Acta Neuropathol 2014; 128: 411–21.

Murray ME, Graff-Radford NR, Ross OA, Petersen RC, Duara R, Dickson DW. Neuropathologically defined subtypes of Alzheimer's disease with distinct clinical characteristics: a retrospective study. Lancet Neurol 2011; 10: 785–96.

Nelson PT, Alafuzoff I, Bigio EH, Bouras C, Braak H, Cairns NJ, et al. Correlation of Alzheimer disease neuropathologic changes with cognitive status: a review of the literature. J Neuropath Exp Neur 2012; 71: 362–81.

Nelson PT, Schmitt FA, Lin YS, Abner EL, Jicha GA, Patel E, et al. Hippocampal sclerosis in advanced age: clinical and pathological features. Brain 2011; 134: 1506–18.

Nelson PT, Smith CD, Abner EL, Wilfred BJ, Wang WX, Neltner JH, et al. Hippocampal sclerosis of aging, a prevalent and high-morbidity brain disease. Acta Neuropathol 2013; 126: 161–77.

Ossenkoppele R, Schonhaut DR, Scholl M, Lockhart SN, Ayakta N, Baker SL, et al. Tau PET patterns mirror clinical and neuroanatomical variability in Alzheimer's disease. Brain 2016; 139: 1551–67.

Pao WC, Dickson DW, Crook JE, Finch NA, Rademakers R, Graff-Radford NR. Hippocampal sclerosis in the elderly genetic and pathologic findings, some mimicking Alzheimer disease clinically. Alzheimer Dis Assoc Disord 2011; 25: 364–8.

Petersen RC, Parisi JE, Dickson DW, Johnson KA, Knopman DS, Boeve BF, et al. Neuropathologic features of amnestic mild cognitive impairment. Arch Neurol 2006; 63: 665–72.

Piguet O, Hornberger M, Mioshi E, Hodges JR. Behavioural-variant frontotemporal dementia: diagnosis, clinical staging, and management. Lancet Neurol 2011; 10: 162–72.

Pontecorvo MJ, Devous MD, Navitsky M, Lu M, Salloway S, Schaerf FW, et al. Relationships between flortaucipir PET tau binding and amyloid burden, clinical diagnosis, age and cognition. Brain 2017; 140: 748–63.

Price CJ, Friston KJ. Cognitive conjunction: a new approach to brain activation experiments. Neuroimage 1997; 5: 261–70.

Price CJ, Moore CJ, Friston KJ. Subtractions, conjunctions, and interactions in experimental design of activation studies. Hum Brain Mapp 1997; 5: 264–72.

Rauramaa T, Pikkarainen M, Englund E, Ince PG, Jellinger K, Paetau A, et al. Consensus recommendations on pathologic changes in the hippocampus: a postmortem multicenter inter-rater study. J Neuropath Exp Neur 2013; 72: 452–61.

Roberts RO, Geda YE, Knopman DS, Cha RH, Pankratz VS, Boeve BF, et al. The Mayo Clinic Study of Aging: design and sampling, participation, baseline measures and sample characteristics. Neuroepidemiology 2008; 30: 58–69.

Senjem ML, Gunter JL, Shiung MM, Petersen RC, Jack CR. Comparison of different methodological implementations of voxel-based morphometry in neurodegenerative disease. Neuroimage 2005; 26: 600–8.

Shcherbinin S, Schwarz AJ, Joshi A, Navitsky M, Flitter M, Shankle WR, et al. Kinetics of the Tau PET tracer 18F-AV-1451 (T807) in subjects with normal cognitive function, mild cognitive impairment, and Alzheimer disease. J Nucl Med 2016; 57: 1535–42.

Tang-Wai DF, Graff-Radford NR, Boeve BF, Dickson DW, Parisi JE, Crook R, et al. Clinical, genetic, and neuropathologic characteristics of posterior cortical atrophy. Neurology 2004; 63: 1168–74.

Terry RD, Hansen LA, Deteresa R, Davies P, Tobias H, Katzman R. Senile dementia of the Alzheimer type without neocortical neurofibrillary tangles. J Neuropathol Exp Neur 1987; 46: 262–8.

Tyas SL, Snowdon DA, Desrosiers MF, Riley KP, Markesbery WR. Healthy ageing in the Nun Study: definition and neuropathologic correlates. Age Ageing 2007; 36: 650–5.

Tzourio-Mazoyer N, Landeau B, Papathanassiou D, Crivello F, Etard O, Delcroix N, et al. Automated anatomical labeling of activations in SPM using a macroscopic anatomical parcellation of the MNI MRI single-subject brain. Neuroimage 2002; 15: 273–89.

Vemuri P, Gunter JL, Senjem ML, Whitwell JL, Kantarci K, Knopman DS, et al. Alzheimer's disease diagnosis in individual subjects using structural MR images: validation studies. Neuroimage 2008; 39: 1186–97.

Xia MR, Wang JH, He Y. BrainNet viewer: a network visualization tool for human brain connectomics. PLoS One 2013; 8: e68910.

Zarow C, Sitzer TE, Chui HC. Understanding hippocampal sclerosis in the elderly: epidemiology, characterization, and diagnostic issues. Curr Neurol Neurosci 2008; 8: 363–70.

Zarow C, Weiner MW, Ellis WG, Chui HC. Prevalence, laterality, and comorbidity of hippocampal sclerosis in an autopsy sample. Brain Behav 2012; 2: 435–42.